Hofmeister Effect in Ion Transport: Reversible Binding of Halide Anions to the Roflamycoin Channel

Pavel A. Grigorjev* and Sergey M. Bezrukov‡§

*Institute of Biological Physics of the Russian Academy of Sciences, Puschino, Russia 142292; ‡St. Petersburg Nuclear Physics Institute of the Russian Academy of Sciences, Gatchina, Russia 188350; and §Division of Intramural Research, National Institute of Diabetes and Digestive and Kidney Disease, National Institutes of Health, Bethesda, Maryland 20892 USA

ABSTRACT We have studied the anion-dependent gating of roflamycoin ion channels using spectral analysis of noise in currents through multichannel planar lipid bilayers. We have found that in addition to low frequency current fluctuations that may be attributed to channel switching between open and closed conformations, roflamycoin channels exhibit a pronounced higher frequency noise indicating that the open channel conductance has substates with short lifetimes. This noise is well described by a Lorentzian spectrum component with a characteristic cutoff frequency that depends on the type of halide anions according to their position in the Hofmeister series. It is suggested that transitions between the substates correspond to a reversible ionization of the channel by a penetrating anion that binds to the channel structure, more chaotropic anions being bound for longer times. Within a framework of a two-substate model, the duration of the substate with reduced electrostatic barrier for cation current varies exponentially with anion electron polarizability. This explains two features of the roflamycoin channel reported earlier: the increase in apparent single-channel conductance along the series $F^- < Cl^- < Br^- < I^-$ and the reverse of channel selectivity from anionic for KF to cationic for KI.

INTRODUCTION

It is well known that ion channels formed in planar lipid bilayers upon the two-sided application of polyene antibiotics, such as amphotericin B or nystatin, are constructed of two semipores, each spanning half of the bilayer thickness (Finkelstein and Holz, 1973; De Kruijff and Demel, 1974; Ermishkin et al., 1977). Lately, the ion channels formed by a new polyene antibiotic, roflamycoin (Fig. 1), were described (Grigorjev et al., 1985). These channels are wider (about 12 Å in diameter) than amphotericin B channels and are supposedly constructed from two semipores, each containing 12–16 roflamycoin molecules and 6–8 sterol molecules. Their parameters appear to be very sensitive to minor changes in the external conditions. Dwell time in the open state, anion to cation selectivity, and conductance of the channel are strongly dependent on the species of penetrating ions, temperature, and membrane potential (Grigorjev et al., 1985). It was shown that single-channel conductance increases along the sequence of the electrolytes KF, KCl, KBr, and KI (Schlegel et al., 1982; Grigorjev et al., 1985). At the same time, the ratio of anion to cation transfer numbers is 4 times less for KI then for KF; in fact, the channel is cation-selective for KI and anion-selective for KF. In addition, it was noticed that the noise of the current through a single open channel is much higher than that of the current baseline (Fig. 2). This observation suggests the existence of poorly resolved fast transitions of the channel between conductance sublevels.

We have studied roflamycoin channels using spectral analysis of spontaneous fluctuations in electric current through a multichannel system (for a preliminary report see Grigorjev and Bezrukov, 1991). We have found that in addition to low frequency current noise related to the channel switching between open and closed states, there is a high frequency Lorentzian noise component with characteristic cutoff frequencies in the range of 100–1000 Hz. The straightforward interpretation of this result is that the open channel has differently conducting substates with short life-times. These life-times depend on the species of the penetrating anions in a way that produces an increase of the average single-channel conductance when F^- is replaced by I^-. This average conductance is measured in single-channel experiments because of time resolution limitations and represents some intermediate value between substates of higher and lower conductance.

It is proposed that the penetrating anion controls gating of the channel substates by binding to the channel structure and reducing the electrostatic barrier for cation current. The duration of the substate of higher conductance correlates with electron polarizability of anions, possibly indicating London-Van-der-Waals interactions of anions with the channel structure. The mean life-time in the state of higher conductance grows in the Hofmeister series $F^- < Cl^- < Br^- < I^-$. Within experimental accuracy, a cation type does not influence gating dynamics. This model explains not only the increase in the apparent single-channel conductance along this series, but also the reverse of channel selectivity from anionic for KF to cationic for KI.

MATERIALS AND METHODS

The polyene antibiotic roflamycoin (Fig. 1) was a generous gift from Dr. R. Schlegel of the Central Institute of Microbiology and Experimental

Received for publication 6 January 1994 and in final form 31 May 1994.

Address reprint requests to Dr. Sergey M. Bezrukov, National Institutes of Health, Bldg. 5, Rm. 405, Bethesda, MD 20892. Tel.: 301-402-4701; Fax: 301-496-0201; E-mail: bezrukov@helix.nih.gov.

0006-3495/94/12/2265/07 $2.00

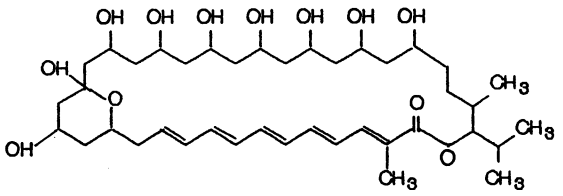

FIGURE 1 Structural formula of polyene antibiotic roflamycoin.

Therapy (Jena, Germany). This antifungal antibiotic is produced by *Streptomyces roseoflavus* JA 5068 (Schlegel and Thrum, 1971). The bilayer membranes were formed using standard techniques (Mueller et al., 1963; Ermishkin et al., 1977) on a circular aperture with 0.2 mm diameter in a Teflon cell immersed into salt water solution. Total ox brain phospholipids dissolved in heptane were used. The sterol concentration of 9% was obtained by adding sterol to the lipid solution. Unbuffered aqueous solutions of electrolytes at 20°C and pH 5.6 ± 0.2 were used. Stock solutions of roflamycoin were prepared by dissolving crystalline samples in dimethylsulfoxide.

Single-channel membrane currents were measured by a Keithly 301 operational electrometer. The output was directly connected to an "X-Y" chart recorder with 0.1 s time resolution. In noise measurements performed on multichannel bilayers, the signal picked up by the Ag/AgCl electrodes was amplified by a low-noise preamplifier and then analyzed with the help of a custom-made multichannel analog spectrum analyzer (Bezrukov et al., 1986a). It has 13 parallel channels, each channel comprising an active bandpass filter, a quadratic detector, and an averaging integrator. The central frequencies of filter bands (f_n) were chosen to obey the relationships $\log(f_{n+1}/f_n) = 0.25$, thus splitting the frequency range 3–3000 Hz equidistantly in logarithmic scale. The accuracy of the spectral measurements in this frequency range was better than 7% at 200 s of averaging time. Measuring the spectral density of current noise with a comparable accuracy at lower frequencies (down to 0.1 Hz) took much longer averaging time. In this case, the drift of the multichannel membrane conductance in time became a serious accuracy-limiting factor, so that we mostly restricted ourselves to studies in the 3–3000 Hz frequency range.

RESULTS AND DISCUSSION

An example of the single-channel current steps obtained with the help of the chart recorder is shown in Fig. 2. It is clear from the figure that the noise of the "flat" part of the current pulses is much higher than the noise of the baseline corresponding to the membrane leakage current. The obtained

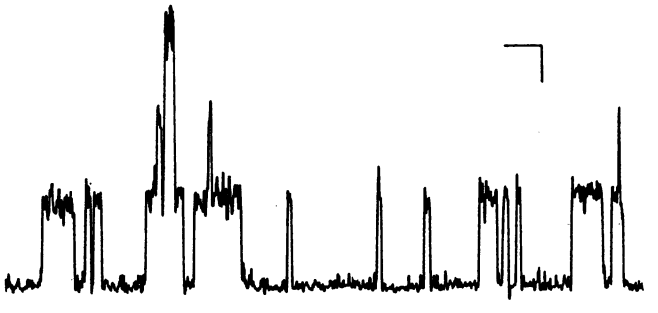

FIGURE 2 Currents through ion channels formed by roflamycoin in the lipid bilayer. The current through a single open channel equals 7.0 ± 0.4 pA. Several segments of the recording show two or three channels open simultaneously. Note that the noise in the current through open channels exceeds the background noise level. Conditions: 1.0 M KBr, applied voltage 100 mV, T = 20°C, time resolution 0.1 s. Calibration: vertical bar, 3×10^{-12} A; horizontal bar, 3 s.

TABLE 1 Conductance of the roflamycoin channel measured in single-channel experiments with different 1 M potassium halides at 100 mV and parameters of the power spectra densities shown in Fig. 4

	$\langle h_i \rangle$ (pS)	$S_{if}(0)$ (A^2 s)	f_f (Hz)
KI	90 ± 6	(2.1 ± 0.2) 10^{-25}	100 ± 10
KBr	70 ± 4	(1.4 ± 0.1) 10^{-26}	440 ± 40
KCl	57 ± 3	(1.0 ± 0.1) 10^{-26}	570 ± 60
KF	39 ± 1.5	(1.7 ± 0.3) 10^{-27}	970 ± 140

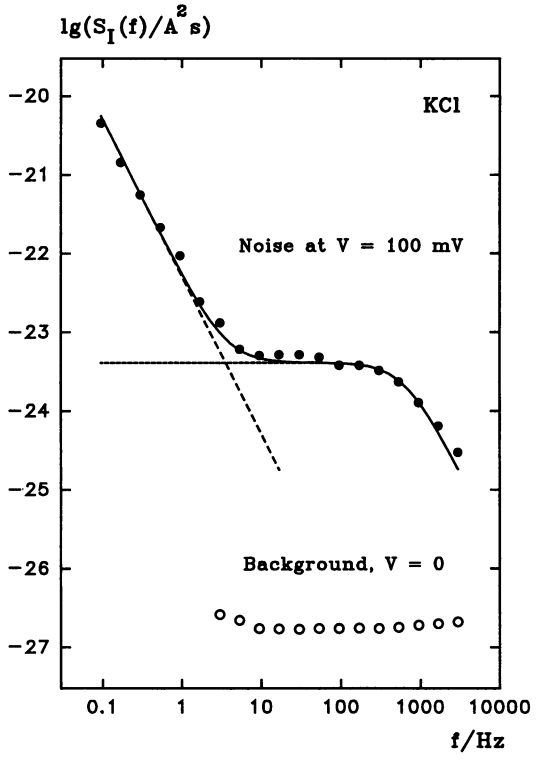

FIGURE 3 Power spectral density, $S_I(f)$, of the current fluctuations generated by the multichannel membrane in 1 M KCl aqueous solution at 100 mV (●) and zero applied voltage (○). The mean membrane conductance was 2.4×10^{-8} S, T = 20°C. Points are the experimental values; the continuous line is drawn according to Eq. 1. "Fast" Lorentzian is seen at frequencies from 3 to 3000 Hz, and the tail of the "slow" Lorentzian is resolved at lower frequencies.

apparent single-channel conductances in 1 M KF, KCl, KBr, KI salts increase from 39 pS for KF to 90 pS for KI at 100 mV and 20°C (Table 1). It was shown (Grigorjev et al., 1985) that the ratio of anion to cation transfer numbers diminishes along this series and is about 4 times less for KI than for KF.

Power spectral density, $S_I(f)$, of the current fluctuations of the membrane with many roflamycoin channels in 1 M KCl and at 100 mV together with the background measured from the same membrane at zero transmembrane voltage is shown in Fig. 3. The background spectrum is a sum of contributions from different sources such as electronics, electrolyte, electrodes, the membrane itself, but mostly it represents the Johnson noise of a feedback resistor. For a 10^7 Ohm resistor that was used throughout multichannel measurements, the spec-

tral density of this noise equals 1.62×10^{-27} A²/Hz. Because of the low level of the background, we neglected its contribution to multichannel noise at 100 mV.

The continuous line in Fig. 3 is a sum of the two Lorentzians describing slow and fast fluctuation processes:

$$S_I(f) = \frac{S_{Is}(0)}{1 + (f/f_s)^2} + \frac{S_{If}(0)}{1 + (f/f_f)^2}. \quad (1)$$

Parameters of the fast process Lorentzian, $S_{If}(0) = 4.1 \times 10^{-24}$ A²/Hz and $f_f = 610$ Hz, describe power spectral density at the limit of zero frequency and the corner (cutoff) frequency of the process, respectively. For the slow process Lorentzian that does not show a pronounced saturation in this frequency range, only a combination of parameters, $S_{Is}(0)f_s^2 = 5.1 \times 10^{-23}$ A² Hz, can be evaluated. Still, it is clear that the corner frequencies of the two Lorentzians differ by more then three orders of magnitude, indicating two separate phenomena as their origin. The slow process and the lower frequency Lorentzian may be attributed to channel transitions between open and closed states (Fig. 2), whereas the higher frequency spectral component suggests the existence of fast sublevels in open channel conductance. We do not see any measurable contribution from $1/f$ noise here. The low frequency part of the spectrum is well described by the $1/f^2$ dependence (*dashed line*), suggesting that it represents a slow exponential relaxation process rather than $1/f$ noise. The same type of power spectra from multichannel bilayers were found for other potassium halides and also for LiCl and RbCl membrane-bathing solutions (data not shown in the figure).

In the present paper, we restrict ourselves to the studies of the fast process only. To account for different numbers of channels in particular membranes, we recalculated power spectral densities obtained from multichannel membranes to a single channel using the following relation:

$$S_i(f) = S_I(f)\langle h_t\rangle/g. \quad (2)$$

Here, $\langle h_t\rangle$ is the channel conductance measured in single-channel experiments with a time resolution of 0.1 s and g is the multichannel membrane conductance. Recalculated noise spectra for KF, KCl, KBr, and KI electrolytes are shown in Fig. 4. The solid lines represent Lorentzians that fit the experimental points with parameters given in Table 1 together with values of $\langle h_t\rangle$.

The correlation between anion transfer numbers and characteristic corner frequencies of the fast process for potassium halides is shown in Fig. 5. It can be seen that both channel anionic selectivity and the fast process rate decrease along the Hofmeister series $F^- > Cl^- > Br^- > I^-$ (Collins and Washabaugh, 1985). The chaotropic species slow down the fast process and induce cationic selectivity.

The intensity of anion-sensitive noise is much higher than that of the shot-noise anticipated for these currents (Heinemann and Sigworth, 1990), but is close to the magnitude of the ionization noise recently reported for α-toxin channels (Bezrukov and Kasianowicz, 1993). Under close conditions, the reversible protonation of α-toxin channels at pH 6.0 gives excess noise with a low frequency spectral density of about 3×10^{-27} A²/Hz per single channel in 1 M NaCl. This value compares well with the present data, especially in the case of KCl and KF membrane-bathing solutions.

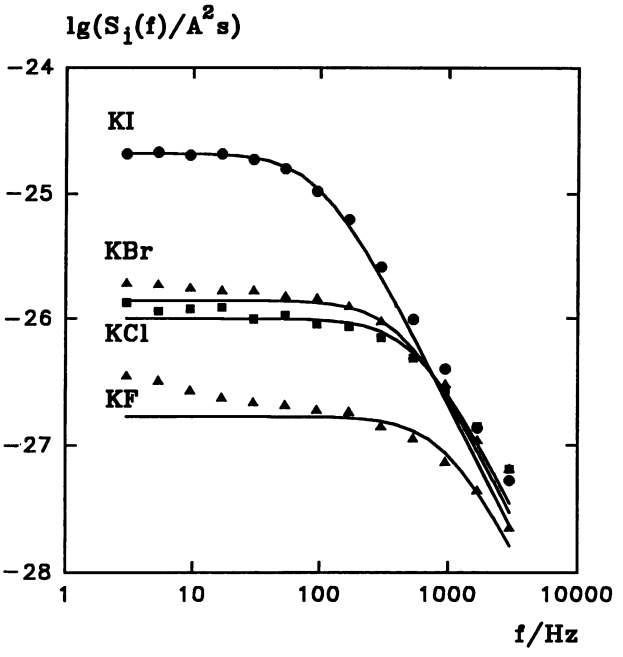

FIGURE 4 Power spectral densities, $S_i(f)$, of the current fluctuations recalculated to a single open roflamycoin channel in 1 M of KF, KCl, KBr, and KI. The continuous lines are Lorentzians drawn with parameters specified in Table 1. Membrane voltage was 100 mV, T = 20°C.

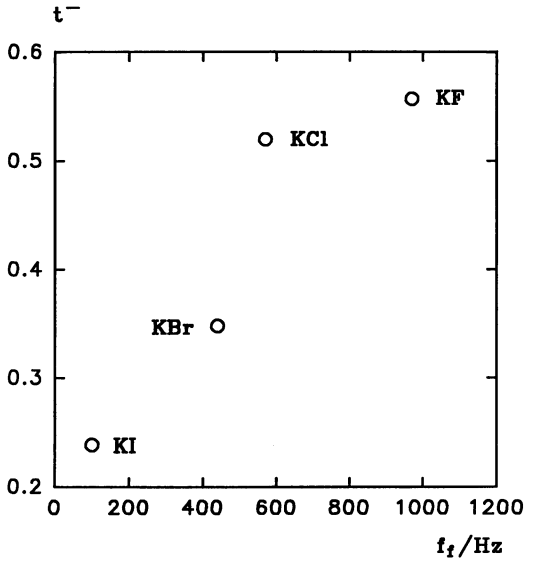

FIGURE 5 Correlation between channel anion transfer numbers and characteristic corner frequencies of the fast process for different potassium halides. Chaotropic anions slow down channel dynamics and introduce cationic specificity.

The simplest model accounting for our results is schematically shown in Fig. 6. It presents single-channel conductance as a function of time. We suggest that the channel has at least two substates of different conductance that are designated by l (low conductance open substate) and h (high conductance open substate). Total dwell-time in the open state, during which the channel performs fast transitions between substates of high and low conductance, is τ_o (we assume that these transitions are described by a two-state Markov process); τ_l and τ_h are dwell-times of the channel in these substates. The mean value of total conductance of the single channel is $\langle h_t \rangle$ and it corresponds to single-channel current directly recorded with the time resolution of the chart recorder (0.1 s); h_s is the amplitude of the transition between the closed state and the low conductance substate ("slow transition"), h_f and $\langle h_f \rangle$ are the amplitude and the mean value of conductance in the l-h transition ("fast transition"). In this model, $\langle h_t \rangle = h_s + \langle h_f \rangle$. The amplitude of h_s is completely resolved in the single-channel experiments (because τ_o is much greater than the time resolution of the chart recorder) and is an additive part of the $\langle h_t \rangle$ registered in these experiments.

As can be seen from the schematic representation of single-channel time behavior in Fig. 6, five parameters are necessary for the complete description of this model. We restrict ourselves only to high frequency l-h transitions, studying the noise of the flat part of the current impulse. For this purpose we will use only "fast" Lorentzians: the Lorentzians with corner frequencies in the range from 100 to 1000 Hz. The slow process of the channel transitions into the open state and back will not be considered in the present paper, so that the number of model parameters is reduced by one (τ_o).

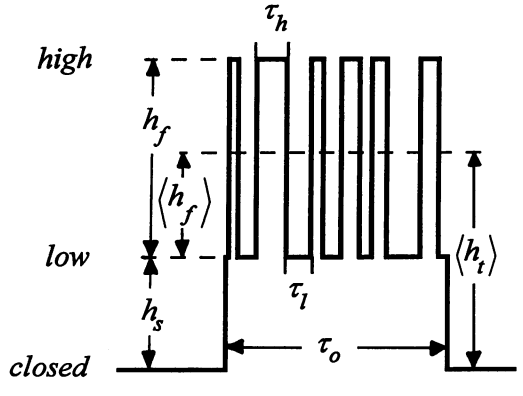

FIGURE 6 Schematic representation of the single-channel conductance. The channel can adopt two conductive substates and a closed (nonconductive) state; h_f is the amplitude of the conductance change caused by the "fast" transitions between substates of low and high conductance; h_s is amplitude of the "slow" conductance change caused by transition between the closed state and the low conductance substate; $\langle h_f \rangle$ is the mean value of the "fast" conductance fluctuations; $\langle h_t \rangle$ is the mean value of the total channel conductance, which corresponds to the experimentally recorded single-channel current with time resolution of 0.1 s (see Fig. 2); τ_h is the mean life time in the high conductance substate, and τ_l is the mean life time in the low conductance substate.

The value $\langle h_f \rangle$ can be expressed through the model parameters in the following way:

$$\langle h_f \rangle = \langle h_t \rangle - h_s = h_f \tau_h / (\tau_h + \tau_t). \quad (3)$$

Additional relationships between the model parameters and the experimentally measured values of $S_i(f)$ and τ_f (τ_f is defined from the corner frequency of the fast Lorentzian according to $\tau_f = 1/2\pi f_f$) can be written in the form (Machlup, 1954; Verveen and DeFelice, 1974; Bezrukov et al., 1986b):

$$S_{if}(0) = 4h_f^2 V^2 \tau_f^2 / (\tau_h + \tau_t), \quad (4)$$

$$\tau_f = \tau_h \tau_t / (\tau_h + \tau_t), \quad (5)$$

where $S_{if}(0)$ is the low frequency limit of the fast Lorentzian noise spectrum component (shown in Fig. 4 by solid lines) and V is transmembrane voltage.

Thus, we have three experimentally obtainable combinations: $h_s + \langle h_f \rangle$, $S_{if}(0)$, and τ_f, for determination of the four remaining model parameters: h_s, h_f, τ_l, and τ_h. This means that the system of Eqs. 3–5 is incomplete. However, the correlation between experimental values of $\langle h_t \rangle$ for KF, KCl, KBr, and KI solutions and the values of the polarizabilities of the anions F^-, Cl^-, Br^-, and I^- helps to solve the problem. This correlation is shown in Fig. 7, suggesting a linear dependence of $\log(\langle h_t \rangle)$ on the polarizability, α_a, of the transferred anions. The linear extrapolation of this function to zero polarizability gives a magnitude of 36 pS. If we assume that the h_s component of the channel conductance in $\langle h_t \rangle = h_s + \langle h_f \rangle$ remains

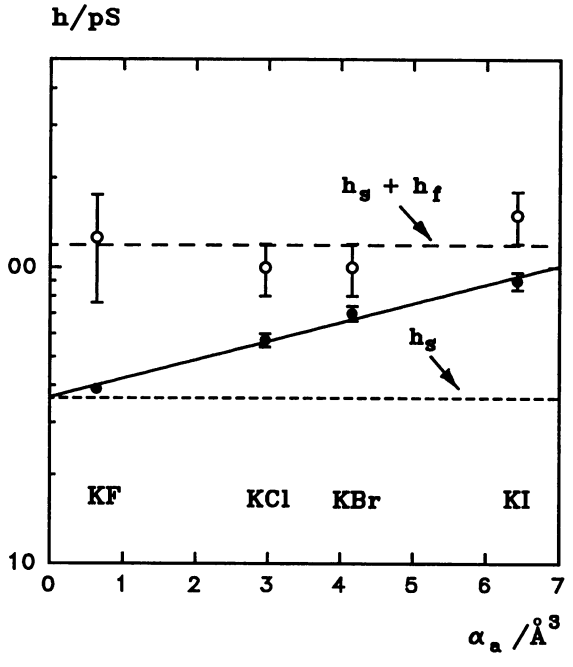

FIGURE 7 Correlation between mean conductance of a single channel, $\langle h_t \rangle$, obtained for different potassium halides by the direct measurement of single-channel currents with the time resolution of 0.1 s (●) and polarizabilities, α_a, of the penetrating anions. The amplitude of the high conductance substate, $h_s + h_f$, recovered by noise spectral analysis is presented by hollow circles. Conditions are the same as for Fig. 4.

constant for all electrolytes, then $\langle h_f \rangle$ can be easily obtained from the single-channel data.

In this case, the three model parameters, h_f, τ_l, and τ_h, can be determined from Eqs. 3–5 in the following manner:

$$h_f = \langle h_f \rangle + S_{if}(0)/(4V^2\langle h_f \rangle \tau_f), \quad (6)$$

$$\tau_h = \tau_f + 4V^2\langle h_f \rangle^2 \tau_f^2 / S_{if}(0), \quad (7)$$

$$\tau_t = \tau_f + S_{if}(0)/(4V^2\langle h_f \rangle^2). \quad (8)$$

Values of $\langle h_f \rangle$ and calculated model parameters, h_f, h_t, τ_l, and τ_h, are given for potassium salts in Table 2, Fig. 7, and Fig. 8. The data on chlorides of Li, Na, and Rb are summarized in Tables 3 and 4. The results show that τ_h is an exponential function of anion polarizability, α_a, and increases by more than an order of magnitude as polarizability grows from 0.64 Å^3 for F^- to 6.43 Å^3 for I^-. The maximum single-channel conductance, $h_s + h_t$, is shown in Fig. 7 and Table 4. This conductance is virtually unchanged along the K^+ row, but increases in the Cl^- column along the sequence Li^+, Na^+, K^+, and Rb^+. Our data also show that the dynamics of the fast transitions of the roflamycoin channels depend strongly upon the species of the penetrating anion and do not depend on the species of the cation (Table 3).

Presented results indicate that the value of the polarizability of the anion is the main parameter governing the dynamics of the fast transitions. We suggest that the anion hopping onto and off a certain site on the channel changes the electrostatic barrier for cations and, correspondingly, channel conductance. The duration of this conductance increase follows the Hofmeister series and might be related to a London-Van-der-Waals type of interaction between the anion and the site, as proposed by Collins and Washabaugh (1985) for Sephadex gels.

There are interesting parallels between findings of the present study and the results on halide ion adsorption reported by these authors (Washabaugh and Collins, 1986). They used aqueous column chromatography on the size exclusion Sephadex G-10 gel (cross-linked dextran) and found that anions adsorb onto the gel according to their position in the Hofmeister series, with the most chaotropic species adsorbing more strongly. The relative elution positions of halide anions were found to be 3.2 for I^-, 1.2 for Br^-, 0.65 for Cl^-, and 0.41 for F^-. These data are in a surprisingly good correspondence with the roflamycoin channel dwell-time in the substate of higher conductance reported here (Fig. 8).

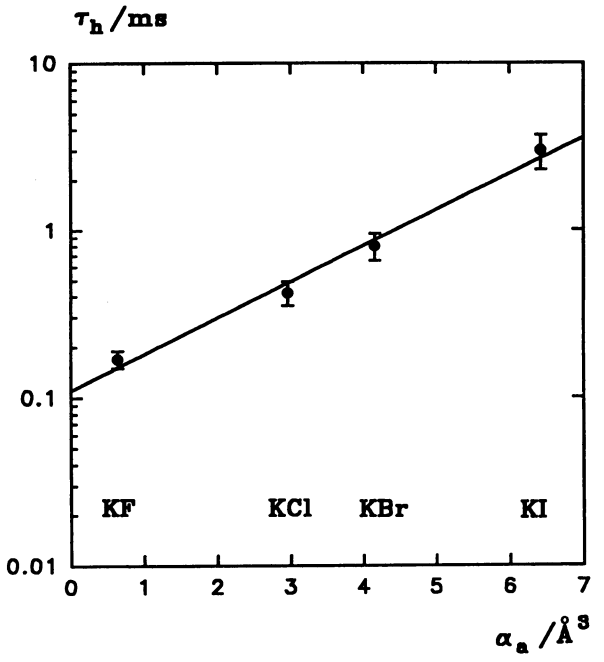

FIGURE 8 Correlation between mean life time of the channel in the substate of higher conductance, τ_h, and polarizabilities, α_a, of the penetrating anions. Chaotropic anions bind to the channel structure for longer times. Conditions are the same as for Fig. 4.

TABLE 3 The corner frequencies, f_c (Hz), of the fast components in noise power spectrum densities for 1 M electrolytes

	F^-	Cl^-	Br^-	I^-
Li^+		540 ± 30		
Na^+		550		
K^+	970 ± 50	570 ± 30	440 ± 20	100 ± 5
Rb^+		600 ± 30		

The correlation between halide anion binding to the roflamycoin channel and anion polarizability found in the present study does not necessarily mean that London dispersion forces are solely (or even mostly) responsible for the binding. Good correlation could also be obtained with water entropy changes caused by different halide anions (Samoilov, 1972) or, simply, with anion size. Importance of anion polarizability in ion interaction with biological structures is questionable (Collins and Washabaugh, 1985). The same is true for anion solvation properties. Results of recent molecular dynamics simulations of small water clusters around Cl^- ions

TABLE 2 Parameters of the model (Fig. 5) deduced from fluctuation analysis and polarizabilities of halide anions

	$\langle h_f \rangle$ (pS)	h_f (pS)	h_t (pS)	τ_h (ms)	τ_t (ms)	α_a* (Å^3)
KI	54 ± 6	115 ± 30	150 ± 30	3.0 ± 0.7	3.4 ± 0.8	6.43
KBr	34 ± 4	63 ± 20	100 ± 20	0.8 ± 0.15	0.7 ± 0.2	4.16
KCl	21 ± 3	64 ± 20	100 ± 20	0.42 ± 0.07	0.8 ± 0.2	2.96
KF	3 ± 1.5	90 ± 50	130 ± 50	0.17 ± 0.02	3.6 ± 2.6	0.64

* Collins and Washabaugh (1985).

TABLE 4 Amplitude of the single roflamycoin channel in the high conductance substate, $h_t = h_s + h_f$ (pS), recovered by fluctuation analysis

	F^-	Cl^-	Br^-	I^-
Li^+		38		
Na^+		50		
K^+	130 ± 50	100 ± 20	100 ± 20	150 ± 30
Rb^+		140 ± 30		

at the changing ion polarizability are controversial (compare data of Perera and Berkowitz (1992) with those of Dang and Smith (1993)). Many factors may contribute to anion binding properties. Still, for the purposes of the present study, we have chosen polarizability as the variable to measure differences between halide anions; it gives not only the right sequence of binding times, but also describes them quantitatively (Fig. 8) in a way expected from energy considerations.

Our model explains how the change in the ratio $\tau_h/(\tau_h + \tau_l)$ affects the magnitude of $\langle h_f \rangle$ and, as a result, the apparent conductance of the channel. The true amplitude of the channel conductance, $h_s + h_f$, does not depend on anion polarizability appreciably (Table 4 and Fig. 7). Conductance amplitude changes with the species of the penetrating cation; the action of the anion mostly consists of the polarizability-dependent gating of the channel.

The model-derived value of h_f is rather sensitive to the choice of h_s, especially in the case of KF. Although this model parameter was not measured directly, it was obtained from experimental data by extrapolation of averaged single-channel conductances in different potassium halides to zero anion polarizability in a semilogarithmic scale (Fig. 7). First, it should be noted here that the result of extrapolation may depend on the type of regression that is used to fit the data. For example, a linear regression for the same single-channel conductances plotted in a linear scale gives a somewhat smaller value for h_s, and, as a consequence, a 35% smaller amplitude of the high conductance state, $h_s + h_f$, in KF salt. Second, even as anion polarizability goes to zero, τ_h approaches some finite value (Fig. 8), which means that the channel still spends a fraction of its time in the higher conductance state. This introduces an additional small (about 2%) shift to the h_s estimate. Nevertheless, these possible corrections to the amplitudes of channel substates do not affect the main conclusions of the present paper.

Our results also suggest a simple explanation for the gradual reduction of anion selectivity along the series KF, KCl, KBr, and KI (Fig. 5). As binding of anions to the channel structure becomes stronger and the dwell-time in the substate of higher conductance grows, the channel develops cationic selectivity because of the reduction of the electrostatic barrier for cations. Weak initial anionic selectivity of the channel in KF solutions becomes suppressed by cationic transport in KI solutions. Moreover, a strong temperature dependence of the roflamycoin channel selectivity now can be readily explained. It was found (Grigorjev et al., 1985) that the ratio of potassium to chloride transfer numbers changed from 0.9 at 21°C to 4.4 at 6°C. According to our model, this means that "the gates" for cations are opened longer at lower temperatures. Indeed, we observed that the corner frequency of the Lorentzian in the case of 1 M KCl decreases from 570 Hz at 20°C to 96 Hz at 11°C.

It can be seen that the two-state ionization model we use to interpret noise data also satisfactorily describes channel transport properties, at least at a qualitative level. Our results suggest that ion transport through the roflamycoin channel is *directly regulated by the reversible ionization* of the channel structure by anion binding. This possibility was proposed earlier by Prod'hom et al. (1987), who studied the dynamics of the dihydropyridine-sensitive Ca^{2+} channel transitions between conducting sublevels (differing by about 70 pS) at changing pH. However, based on additional experimental evidence, these authors concluded later that the observed conductance change reflects an intrinsic conformational transition in the structure of the channel protein that is facilitated by the channel protonation (Hess et al., 1989).

Recently, a fluctuation analysis of the reversible protonation of a single α-toxin channel produced strong evidence supporting the idea of direct electrostatic action of a bound ion as a mechanism of channel regulation (Bezrukov and Kasianowicz, 1993). It was shown that the multiple site ionization is responsible for the change in channel conductance at varying pH. The conductance increment, recalculated to a single ionization event, is about 30 pS for 1.0 M aqueous sodium chloride solutions and, as one would expect for ionization with the Debye screening, decreases at raising salt concentrations. In the present paper, we show that gating dynamics of the roflamycoin channel conductance sublevels (differing by about 60 pS for 1.0 M potassium chloride) correlate with polarizability of penetrating halide anions according to their positions in the Hofmeister series. Combined with the data on ion selectivity changes (Fig. 5), our findings point to the ionization model of channel regulation.

We would like to thank Drs. V. A. Parsegian, I. Vodyanoy, D. C. Rau, J. J. Kasianowicz, and I. B. Golovanov for fruitful discussion of the results and helpful suggestions.

REFERENCES

Bezrukov, S. M., and J. J. Kasianowicz. 1993. Current noise reveals protonation kinetics and number of ionizable sites in an open protein ion channel. *Phys. Rev. Lett.* 70:2352–2355.

Bezrukov, S. M., G. M. Drabkin, and A. I. Sibilev. 1986a. Conductance fluctuations in the laminar flow of a colloid. *J. Colloid Interface Sci.* 113:194–202.

Bezrukov, S. M., V. G. Pokrovskii, and Yu. V. Natochin. 1986b. Mechanism of stimulation of sodium channels with cobalt ions in apical membrane of frog skin cells (fluctuation analysis). *Doklady Biophys.* 286/287/288: 307–310.

Collins, K. D., and M. W. Washabaugh. 1985. The Hofmeister effect and the behavior of water at interfaces. *Q. Rev. Biophys.* 18:323–422.

Dang, L. X., and D. E. Smith. 1993. Molecular dynamics simulations of aqueous ionic clusters using polarizable water. *J. Chem. Phys.* 99: 6950–6956.

de Kruijff, B., and R. A. Demel. 1974. Polyene antibiotic—sterol interactions in membranes of *Acholeplasma Laidlawii* cells and lecithin liposomes. III. Molecular structure of the polyene antibiotic-cholesterol complexes. *Biochim. Biophys. Acta.* 339:57–70.

Ermishkin, L. N., Kh. M. Kasumov, and V. M. Potzeluev. 1977. Properties of Amphotericin B channels in a lipid bilayer. *Biochim. Biophys. Acta.* 470:357–367.

Finkelstein, A., and R. Holz. 1973. Aqueous pores created in thin lipid membranes by the polyene antibiotics nystatin and amphotericin B. *In* Membranes. Vol. 2. Lipid Bilayers and Antibiotics. G. Eisenman, editor. Marcel Dekker, New York. 377 pp.

Grigorjev, P. A., and S. M. Bezrukov. 1991. Roflamycoin channels in the lipid bilayer. *Biophys. J.* 59:459*a*. (Abstr.)

Grigorjev, P. A., R. Schlegel, H. Thrum, and L. N. Ermishkin. 1985. Roflamycoin—a new channel-forming polyene antibiotic. *Biochim. Biophys. Acta.* 821:297–304.

Heinemann, S. H., and F. J. Sigworth. 1990. Open channel noise. V. Fluctuating barriers to ion entry in gramicidin A channels. *Biophys. J.* 57: 499–514.

Hess, P., B. Prod'hom, and D. Pietrobon. 1989. Mechanism of interaction of permeant ions and protons with dihydropyridine-sensitive calcium channels. *Ann. N. Y. Acad. Sci.* 560:80–93.

Machlup, S. 1954. Noise in semiconductors: spectrum of a two-parameter random signal. *J. Appl. Phys.* 25:341–343.

Mueller, P., D. O. Rudin, H. T. Tien, and W. C. Wescott. 1963. Methods for the formation of single bimolecular lipid membranes in aqueous solution. *J. Phys. Chem.* 67:534–535.

Perera, L., and M. L. Berkowitz. 1992. Structure and dynamics of $Cl^-(H_2O)_{20}$ clusters: the effect of the polarizability and the charge of the ion. *J. Chem. Phys.* 96:8288–8294.

Prod'hom, B, D. Pietrobon, and P. Hess. 1987. Direct measurement of proton transfer rates to a group controlling the dihydropyridine-sensitive Ca^{2+} channel. *Nature.* 329:243–246.

Samoilov, O. Ya. 1972. Residence times of ionic hydration. *In* Water, and Aqueous Solutions. Structure, Thermodynamics, and Transport Processes. R. A. Horne, editor. Wiley-Interscience, New York. 597–612.

Schlegel, R., and H. Thrum. 1971. A new polyene antibiotic, flavomycoin. Structural investigations. *J. Antibiot.* 24:360–374.

Schlegel, R., P. A. Grigorjev, and H. Thrum. 1982. Single ionic channels in lipid bilayers formed by roflamycoin, an anti fungal carbonyl conjugated pentaene antibiotic. *Studia biophys.* 92:135–140.

Verveen, A. A., and L. J. DeFelice. 1974. Membrane noise. *Prog. Biophys. Mol. Biol.* 28:189–265.

Washabaugh, M. W., and K. D. Collins. 1986. The systematic characterization by aqueous column chromatography of solutes which affect protein stability. *J. Biol. Chem.* 261:12477–12485.